# Simulation study of the glass transition temperature in poly(methyl methacrylate)

Mesfin Tsige and P. L. Taylor

*Department of Physics, Case Western Reserve University, Cleveland, Ohio 44106-7079*

The glass transition in syndiotactic poly (methyl methacrylate) has been studied through atomistic molecular dynamics simulations performed at temperatures in the range from 297 K to 684 K. The mean squared deviations of atoms, monomers, and molecules from their initial positions were analyzed by means of a technique that separates the effects of diffusive motion from the underlying vibrational motion. The diffusive motion shows a novel power-law variation with time, with an exponent that varies continuously from 0.5 below the glass transition temperature $T_g$ to 1 at high temperatures. The self part of the van Hove correlation functions for both hydrogen atoms and monomers shows structural arrest at the lowest temperature studied. A second peak in the atomic van Hove correlation is attributed to rotation of the $CH_3$ group.

## I. INTRODUCTION

The phenomenon known as the glass transition can be characterized in a wide variety of ways. A changeover in behavior from that typical of a disordered solid to one more akin to a liquid occurs as the temperature is raised in a large number of amorphous materials [1]. The fact that this change happens in a very narrow temperature range has led to its description as a transition, even though there is little evidence that it can be considered a true phase transition in the thermodynamic sense.

The plexus of changes observed at the glass transition can be divided into two families. One set involves measurements made in equilibrium, while the other is concerned with the response to externally imposed stimuli that remove the system from its equilibrium state. The first category includes changes in macroscopic properties such as thermal expansion and heat capacity or in such microscopic quantities as the temporal variation of the mean squared displacement of individual atoms. The family of nonequilibrium phenomena similarly may be divided into the macroscopic category, which includes viscosity and acoustic attenuation, and microscopic quantities such as drag forces on an atom constrained to move with a specified velocity.

The study of static and dynamic properties of macromolecular glasses is one of the most challenging problems in polymer science [2,3]. It is interesting not only as a result of its role in enabling predictions of the material properties of pure polymers. It is, in addition an essential preliminary to the study of the diffusion of organic materials into polymers in the glassy state.

In this paper we report the results of a study of the glass transition in poly(methyl methacrylate), abbreviated here as PMMA. In order to obtain information regarding structural changes and chain dynamics in the vicinity of the glass transition, we have performed atomistic molecular dynamics simulations. As in all such work, the principal obstacle is the need to run the simulations for a sufficiently long time that accurate results can be achieved. The time scales involved in atomic motions in glasses are so many, and so disparate, that special care must be taken to identify the role of each one in tracking the approach to equilibrium in any simulation.

The shortest time interval $\tau_0$ is that concerned with the reversal of motion of a single atom and is of the order of a picosecond. Its reciprocal $\nu_0$ represents the attempt frequency with which an atom makes an excursion towards the potential barrier created by surrounding bonded and non-bonded atoms. At the lowest of temperatures the motion of all the atoms is generally harmonic, but at higher temperatures anharmonic terms become significant.

As the temperature is raised, the probability increases that an atom or group can surmount the barrier posed by the cage of surrounding atoms, and find itself in a new local environment. This is the beginning of the self-diffusion process, and introduces a new time interval $\tau_1$ that is the reciprocal of this transition probability. While $\tau_0$ is only weakly dependent on temperature, the much longer time $\tau_1$ varies exponentially with the inverse temperature.

Even longer time scales $\tau_2$ are introduced when we look at the collective motion of many atoms that is necessary for a macroscopic system to respond to such stimuli as shear stresses. Finally, a set of time scales is found that are so long that they describe processes essentially never observed. Examples of these range from crystallization to the nuclear fusion of the hydrogen atoms, and lead us to use the term "equilibrium" to refer to the state at which no observable changes occur within experimental timescales.

## II. APPROACH

A number of different methods have been used in the attempt to identify the glass transition in molecular-dynamics simulations. One commonly used approach is to study the change in thermal expansion coefficients in ensembles held at constant particle number, pressure, and temperature [4–6]. All thermal expansion results from anharmonic forces, and so the change in expansion coefficient as one passes from a glassy system, which has many of the characteristics of a disordered solid, to a rubbery system, which is more akin to a constrained liquid, should provide a sensitive measure of the glass transition temperature $T_g$. The difficulty here is that the value of $T_g$ derived in simulations in which the temperature is continuously varied is generally dependent on the rate of cooling [7]. An alternative approach is to examine the

temperature dependence of the mean squared displacement of atoms or molecules in ensembles held at constant particle number, volume, and temperature [8,9].

The most valuable technique with which to study the glass transition by means of simulations will clearly be one that studies behavior over the shortest possible time scale. It will also be valuable to seek the highest precision in the prediction of $T_g$, and to maximize the number of internal controls for self-consistency in the results. For this reason we choose to study the mean squared displacement of atoms from their initial positions. This approach appears to give reproducible and consistent results within a simulated time of the order of the barrier penetration time $\tau_1$.

The previously defined characteristic times, $\tau_0$, $\tau_1$, and $\tau_2$ separate the time intervals from which information may be obtained. In the shortest interval, for which $t \ll \tau_0$, the atomic motion is essentially ballistic. The velocities can be considered constant, and the mean squared deviation of an atom from its initial position increases quadratically with time. We define this mean squared deviation as

$$g(\tau) = \langle [\mathbf{r}(t+\tau) - \mathbf{r}(t)]^2 \rangle, \tag{1}$$

where the average $\langle \cdots \rangle$ is over all atoms and all times t, and where $\mathbf{r}$ is the position of an atom.

As $t$ approaches $\tau_0$, the quasiharmonic restoring forces come into play, and $g(\tau)$ starts to flatten. For a perfect harmonic system $g(\tau)$ would tend to a constant as $\tau$ becomes much larger than $\tau_0$, but in a real glassy system the slope remains small but nonvanishing. At the glass transition we expect some softening of these restoring forces, and so a shift in the location in time of the transition from ballistic to quasiharmonic motion provides the first indicator for $T_g$.

At times larger than $\tau_0$ but smaller than $\tau_1$ the atoms are, for the most part, oscillating about their equilibrium positions. The anharmonic content of this motion increases rapidly as the temperature is raised to approach $T_g$, and this is reflected in both the thermal expansion and the mean squared displacement. The study of this regime has the advantage that long simulation runs are not required, but has the disadvantage that the results are not very sensitive to small changes in temperature. One is detecting the fact that the potential wells in which the atoms move are not parabolic, but exhibit a softening as the amplitude of vibration increases. The atoms may even make excursions into regions in which the curvature of the potential becomes negative. They are unlikely, however, at these early times to surmount the potential maxima and drop into new positions of local equilibrium.

It is in the range of times greater than $\tau_1$ that the most definitive signature of the glass transition can be observed. Diffusion can then occur over significant distances, and so it is the mean squared displacement $g(\tau)$ that is the appropriate object for study in this regime. It does, however, require the greatest computing time, and can be subject to the greatest statistical uncertainties. Nevertheless, self-diffusion is so central to the concept of the glass transition that it is necessary to pay particular attention to this process.

In Sec. III we develop a theoretical model to aid in the interpretation of the results of simulations. In particular, we need to have clear theoretical predictions of the form we expect to be taken by the average squared deviation of an atom from its starting position.

### III. THEORETICAL ANALYSIS

The quantity on which we choose to concentrate is the function $g(\tau)$ defined in Eq. (1). There are three reasons for this choice. First, there is information about the glass transition to be obtained from $g(\tau)$ in all ranges of $\tau$. Second it is a relatively easy quantity to extract from the results of simulations. Third, $g(\tau)$ is approximately related to the results of some experimental measurements.

In the Mössbauer effect, for example, the energy spectrum of emitted $\gamma$ rays is the Fourier transform of a quantity that contains the correlation function $\langle e^{i\mathbf{k}\cdot\mathbf{r}(\tau)} e^{-i\mathbf{k}\cdot\mathbf{r}(0)} \rangle$. If one ignores the quantum-mechanical commutator of $\mathbf{r}(t)$ and $\mathbf{r}(0)$ this becomes $\langle e^{i\mathbf{k}\cdot\mathbf{r}(\tau) - i\mathbf{k}\cdot\mathbf{r}(0)} \rangle$. With the further approximation that the dynamics of the system can be represented as an assembly of harmonic oscillators in thermodynamic equilibrium, the correlation function becomes equal to $\exp(-\frac{1}{2}k^2 \langle [\mathbf{r}(\tau) - \mathbf{r}(0)]^2 \rangle)$ [10].

In order to interpret the form of $g(\tau)$ obtained from simulations or experiment we need a theoretical model capable of exhibiting the principal features found in this function. The model we take is one in which the motion of an atom is dominated by harmonic-oscillator-like vibration. Onto this is superimposed a random displacement $\mathbf{r}_d(t)$ of the center of the oscillator. The displacement is then

$$\mathbf{r}(\tau) = \sum_q \mathbf{r}_q \cos(\omega_q \tau + \phi_q) + \mathbf{r}_d(\tau) \tag{2}$$

with $\mathbf{r}_q$ the component in the mode $q$ of angular frequency $\omega_q$ and phase $\phi_q$, from which

$$\langle [\mathbf{r}(\tau) - \mathbf{r}(0)]^2 \rangle = \left\langle \left[ \mathbf{R}(\tau) + \sum_q 2\mathbf{r}_q \sin\left(\frac{1}{2}\omega_q \tau\right) \right. \right.$$
$$\left. \left. \times \sin\left(\frac{1}{2}\omega_q \tau + \phi_q\right) \right]^2 \right\rangle \tag{3}$$

with $\mathbf{R}(\tau) = \mathbf{r}_d(\tau) - \mathbf{r}_d(0)$. On averaging over the random phases, which is equivalent to integrating over all the various $\phi_q$, all the crossterms vanish, and $\langle \sin^2(\frac{1}{2}\omega_q \tau + \phi_q) \rangle = \frac{1}{2}$. We are then left with

$$\langle [\mathbf{r}(\tau) - \mathbf{r}(0)]^2 \rangle = \langle \mathbf{R}^2(\tau) \rangle + \sum_q \langle \mathbf{r}_q^2 \rangle (1 - \cos \omega_q \tau). \tag{4}$$

Because a glass is inherently disordered, the normal modes will not be traveling waves, and no simple expression for $\mathbf{r}_q$ is available. In a classical Bravais lattice in thermal equilibrium, each normal mode has energy $k_B T$, and so we would have

$$\langle \mathbf{r}_q^2 \rangle = k_B T / M \omega_q^2 N \tag{5}$$

with $k_B$ Boltzmann's constant and $M$ the mass of each of the $N$ atoms in the lattice. For our disordered glass we assume the existence of some average inverse mass $\langle M^{-1} \rangle \equiv m^{-1}$, and replace the sum over $q$ by an integral $\int \mathcal{D}(\omega) d\omega$. Here $\mathcal{D}(\omega)$ is the density of states, defined as the sum over the classical normal modes of vibration given by the expression

$$\mathcal{D}(\omega) = \sum_q \delta(\omega - \omega_q). \tag{6}$$

We then have

$$g(\tau) = \langle \mathbf{R}^2(\tau) \rangle + \frac{k_B T}{mN} \int \frac{\mathcal{D}(\omega)}{\omega^2} (1 - \cos \omega \tau) d\omega. \tag{7}$$

Both terms in this expression describe random displacements of a molecule from its initial position. The first term is associated with slow diffusive motion, while the second is due to motion that is initially more rapid, but which is limited to small distances. At short times $\tau \ll \tau_0$ we can ignore $\mathbf{R}(\tau)$ and expand the cosine to find

$$g(\tau) \simeq \frac{k_B T}{2mN} \int \mathcal{D}(\omega) \left( \tau^2 - \frac{\omega^2 \tau^4}{12} \right) d\omega. \tag{8}$$

This is conveniently written as

$$\frac{g(\tau)}{T\tau^2} \simeq \frac{3k_B}{2m} \left( 1 - \frac{\tau^2}{36N} \int \omega^2 \mathcal{D}(\omega) d\omega \right). \tag{9}$$

When this quantity is plotted as a function of $\tau^2$, its slope at vanishing $\tau^2$ thus gives an approximation to the second moment of the vibrational density of states. Any change in the effective stiffness of the restoring forces of the type to be expected at the glass transition should be observable as a change in this quantity.

At times much larger than $\tau_0$, the oscillatory term in Eq. (5) gives a negligible contribution, and we find

$$g(\tau) = \langle R^2(\tau) \rangle + k_B T / m \omega_D^2, \tag{10}$$

with $\omega_D$ a characteristic frequency that is of the order of the Debye frequency of the polymer. The important point here is that the second term on the right-hand side of Eq. (8) is independent of $\tau$. It can then, in principle, be subtracted from the observed $g(\tau)$ to yield the form of $\langle R^2(\tau) \rangle$, which is the quantity of interest for diffusive processes.

## IV. DETAILS OF THE SIMULATION

Atomistic molecular dynamics is the most straightforward method for studying the motion of individual particles. Its essential elements are the potential energy (i.e. the interaction potential for the particles from which the forces can be calculated) and the equations of motion (Newton's or any other formulation of the classical equations of motion) that govern the dynamics of the particles. Being deterministic, it requires knowledge of the initial positions and velocities of the particles.

Calculating the exact potential energy of a system of molecules is a formidable many-body problem, and so empirical methods are used to represent it as a function of the geometric variables of the atoms involved. The parameters that are important for the calculation of the potential energy are determined using experimental and quantum-mechanical methods, and the equations and parameters used to define it are commonly called a force field.

In general, force fields are developed to handle specific classes of molecules. In the case of atomistic molecular dynamics simulations the force fields used commonly represent each atom in the system as a single point, and energies as a sum of two-, three-, and four-particle interactions. The available atomistic force fields differ in the functional form of the equations and in the parameter sets used in defining the potential energy surface, and tend to perform best for molecular systems similar to those used in their parameterization. The available force fields range from the rather simple Dreiding force field [11] to the more elaborate COMPASS (Condensed-phase Optimized Molecular Potentials for Atomistic Simulation Studies) [12]. This latter force field has several advantages. It avoids, for example, a shortcoming of many other fields in which the parameters are found by fitting room-temperature crystal data to energy minimizations performed at zero temperature. On the other hand, its more elaborate nature and its inclusion of off-diagonal cross-coupling terms make it slower in operation. There is, thus, always a trade-off between simplicity and accuracy in choosing among the available force fields or in developing a new one. In our case, on the basis of our previous experience [13–15] we chose the Dreiding force field applied in the commercial software package [16] CERIUS$^2$ throughout the simulation. Details of the form of the energy terms in the Dreiding force field are given in our previous publications [13–15].

Historically, several different ways of generating the starting set of atomic coordinates for molecular dynamics simulation have been used. For our case, the initial configuration was generated in two steps. First, using the CERIUS$^2$ amorphous builder, 4086 atoms assembled into 18 chains of syndiotactic PMMA of degree of polymerization 15 were enclosed in a cubic cell with a density chosen to be equal to the experimental value. To avoid surface effects, periodic boundary conditions were used. The potential energy was then minimized to produce an initial configuration for the molecular dynamics simulations.

In integrating the equations of motion, a key parameter is the integration time step $\Delta t$. Since it has to be small enough for the fastest modes to be handled accurately, we chose a time step of 2 fs for all simulations. The initial velocities of the atoms were assigned using a Maxwell-Boltzmann distribution at the desired temperature but with the constraint that the velocity of the center of mass of each molecule should be zero. The simulations were carried out at constant number of atoms, constant volume and constant temperature, and each atom was allowed to interact with only the nearest image of each other atom in the periodic array formed by the boundary conditions. The coordinates of each of the atoms were then saved every 1 ps for later analysis.

The simulations were performed in a system held at constant volume. The reason for this choice is that the alternative option of a system at constant pressure requires the determination of a different value of the volume for each temperature studied. Because of the limited size of feasible model systems there are fluctuations in the calculated volume that lead to unacceptable inaccuracies in the calculation of any other property of the system [2]. In order to take advantage of the high precision available in the computation of the mean squared molecular displacements it was, thus, necessary to maintain a fixed volume of the cell in which the polymer was maintained.

There is also another reason for maintaining constant volume that is quite separate from issues of computational precision. If the volume were allowed to increase and a glass transition were observed, it would be unclear whether the phenomenon was merely a consequence of thermal expansion, or whether it was a manifestation of some truly cooperative behavior. By maintaining a constant volume in the simulations we avoid this ambiguity.

It was essential to make sure that the simulated system was equilibrated at all temperatures studied. Particularly at low temperatures the system may not be equilibrated if it is not run beyond the long relaxation times that may exist at these low temperatures. In order to overcome this problem we first annealed our system through range of temperatures for a total of about 5 ns. We then performed long simulation runs of duration up to 1.8 ns at ten different temperatures ranging from 297–684 K. Since the volume was the same at all temperatures, it was not necessary to generate starting configurations at each new temperature. Instead we equilibrated at each new temperature the configuration that was generated and equilibrated at the previous temperature. In order to test that equilibrium had actually been attained at each temperature, we compared average mean squared displacements of the atoms calculated at that given temperature but using different time origins for the 1.8 ns simulation run. If the system is not in equilibrium then the calculated mean squared displacements for that given temperature would show some dependence on the starting time. In our case, the differences among the calculated mean squared displacements at a given temperature were found to be within statistical uncertainty.

## V. RESULTS AND DISCUSSION

*Time dependence of the mean squared displacement*. The overall dynamics of polymeric systems is reflected in their self-diffusion behavior [17]. This can be most conveniently extracted by calculating the mean squared displacement from molecular-dynamics generated trajectories. In our case, since we have information at the atomistic level, we can study the dynamics of our polymer system at different length scales. For this purpose we define three different mean squared displacements, ranging from the atomic to the molecular.

The mean squared displacement of individual atoms is evaluated as

$$g_0(t) = \langle [\mathbf{r}_i(t) - \mathbf{r}_i(0)]^2 \rangle \qquad (11)$$
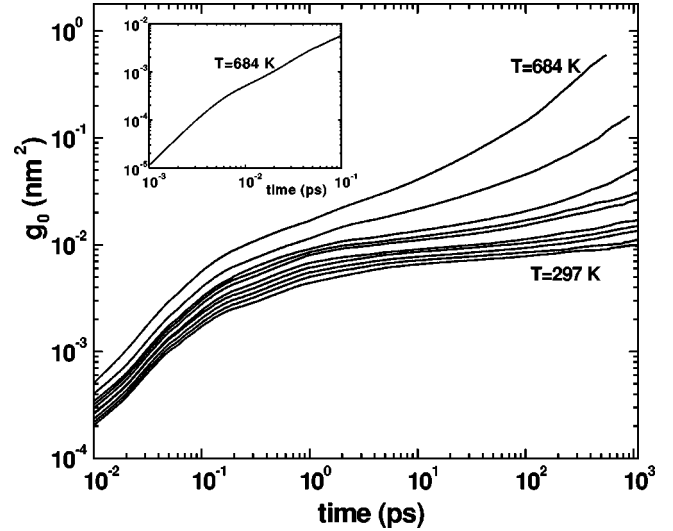


FIG. 1. Atomic mean squared displacement evaluated at ten different temperatures (297, 324, 346, 396, 415, 436, 472, 509, 599, and 684 K). Inset: same quantity at the highest temperature studied but with time starting from 1 fs to show the ballistic region clearly.

where $\mathbf{r}_i(t)$ is the position of the $i$th atom at time t and $\langle \cdots \rangle$ denotes the average for all PMMA constituent atoms as well as for all time origins available within the simulation. Similarly, the mean squared displacement of individual monomers is
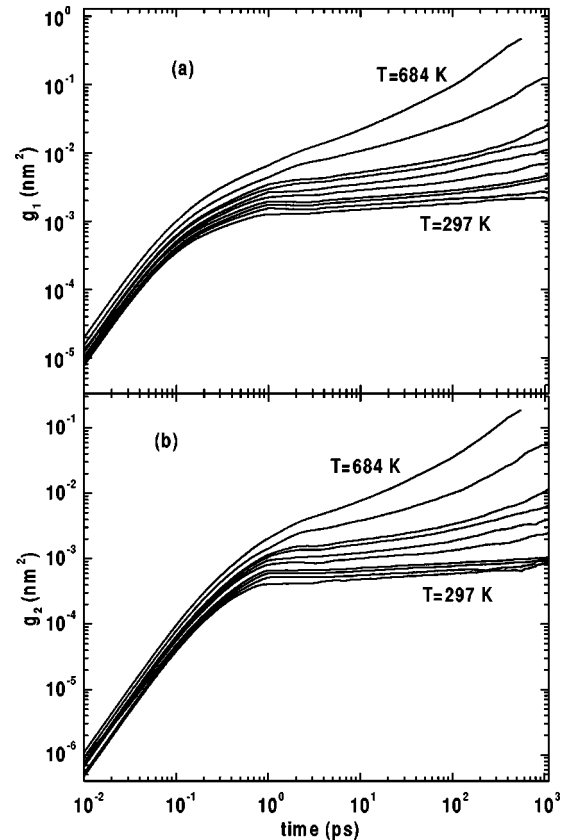


FIG. 2. Mean squared displacements as in Fig. 1, but for displacements of center of mass of (a) monomers and (b) polymers.
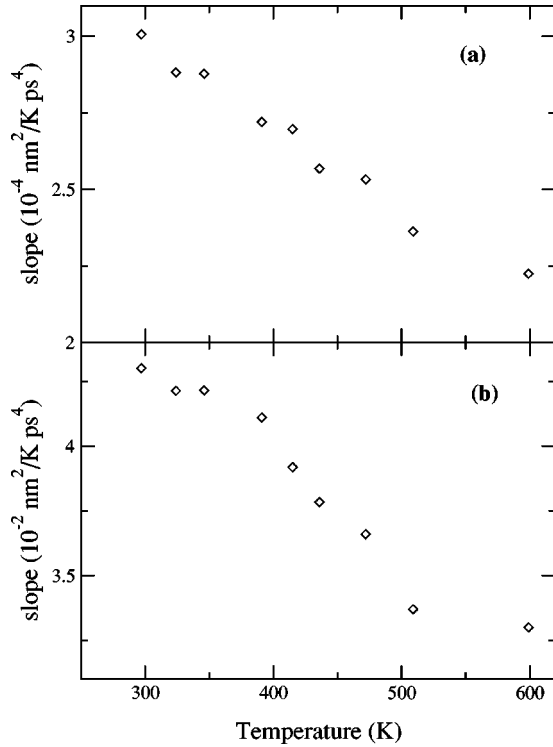
FIG. 3. At short times the mean squared displacement $g_2(\tau)$ of the center of mass of polymer molecules can be expanded in powers of $\tau^2$. Plot (a) shows the initial slope of $g_2(\tau)/T\tau^2$, and is an indication of the softening of phonon modes with temperature. Plot (b) is for the monomeric function $g_1(\tau)/T\tau^2$, and shows possible signs of a change of slope around 400 K.

$$g_1(t) = \langle [\mathbf{r}_{j,k}(t) - \mathbf{r}_{j,k}(0)]^2 \rangle, \qquad (12)$$

where $\mathbf{r}_{j,k}(t)$ is the position of the center of mass of the $j$th monomer in the $k$th molecule. Finally, the average mean squared displacement of individual molecules is

$$g_2(t) = \langle [\mathbf{r}_k(t) - \mathbf{r}_k(0)]^2 \rangle, \qquad (13)$$

where $\mathbf{r}_k(t)$ is the position of the center of mass of the $k$th molecule (polymer chain) at time $t$.

Figure 1 shows the atomic mean squared displacement as a function of time, evaluated at ten different temperatures ranging from 297 K to 684 K. Figure 2 shows the corresponding monomeric and molecular mean squared displacements. As expected, there is an initial ballistic region, during which $g(t)$ grows as $t^2$. This regime lasts for only a few femtoseconds in the case of the atomic displacement described by $g_0(t)$, as the vibrations of the hydrogen atoms are very rapid, and is visible in only the lower left corner of the inset in Fig. 1. The ballistic regime is most pronounced in the molecular mean squared displacement $g_2(t)$ where it persists for hundreds of femtoseconds.

From the data we can examine the softening of the vibrational modes as the temperature is increased. The quantity $g_2(\tau)/T\tau^2$, whose character was suggested in Eq. (7), has the initial slope plotted in Fig. 3(a). These data were obtained from runs of only a few hundred femtoseconds, and thus required computational resources smaller by several orders
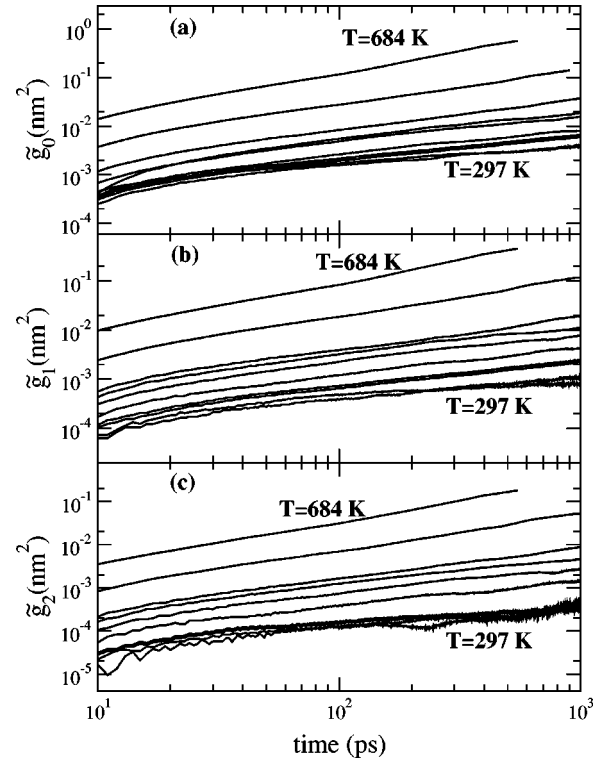


FIG. 4. Reduced mean squared displacements for (a) atomic, (b) monomeric, and (c) polymeric motion. These plots differ from those in Figs. 1 and 2 in that the vibrational contributions have been subtracted.

of magnitude than those needed to examine the diffusive regime. It would thus be highly desirable if information about $T_g$ could be extracted from such brief simulations. A steady decrease with temperature is observed, but unfortunately, no distinctive changes mark the location of $T_g$. Similar data for the initial slope of $g_1(t)/T\tau^2$ are shown in Fig. 3(b). While there is a possible indication of a change in slope of this curve between 350 K and 400 K, the behavior is not pronounced. We thus conclude that to demonstrate the use of mode softening as an indicator of the glass transition will require better statistics than were available from the smaller number of runs that we performed.

As the time increases, and we leave the ballistic region, the curves in Figs. 1 and 2 start to flatten out. For low temperatures the slope of $g(t)$ becomes small in all three cases, but for high temperatures the plots then start to rise again, curving upwards in such a way that no well-defined power law can be assigned. At this point we recall the theoretical analysis, in which it was pointed out in Eq. (8) that $g(t)$ is likely to be the sum of a diffusive term and a constant at times greater than $\tau_0$. It is, thus, appropriate to isolate the diffusive part before making the type of logarithmic plot shown in Figs. 1 and 2. Accordingly the constant terms were identified by extrapolating to zero time the linear regions of $g_0$, $g_1$, and $g_2$ occurring between 10 ps and 40 ps. Subtraction of the numbers given by these intercepts then yields new functions $\tilde{g}_0$, $\tilde{g}_1$, and $\tilde{g}_2$, which we expect to be better representations of the mean squared diffusive displacements $\langle R^2(t) \rangle$. These results are shown in Fig. 4. We see immedi-
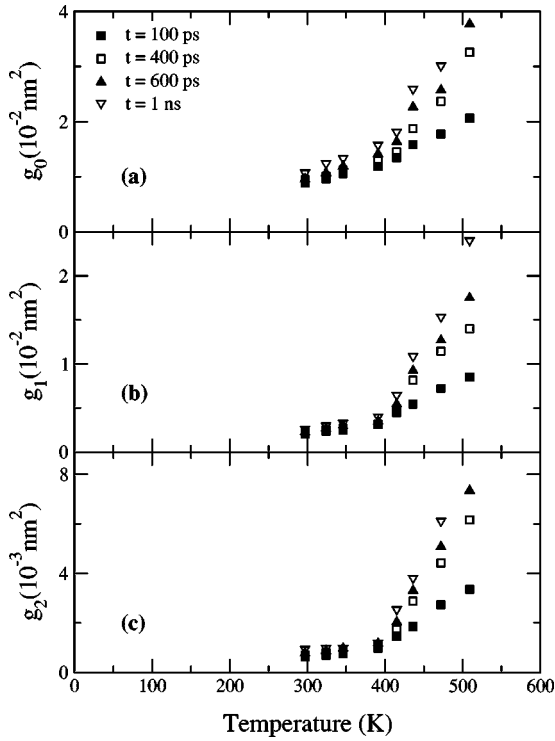
FIG. 5. The three mean squared displacements ($g_0$, $g_1$, and $g_2$) replotted as a function of temperature at four different observation times.



FIG. 6. As in Fig. 5, but for the reduced mean squared displacements $\tilde{g}_0$, $\tilde{g}_1$, and $\tilde{g}_2$.

ately that linearity has been restored to these curves in this log-log plot, showing that the diffusive component of the mean squared displacement is following a power law with time when $t \gg \tau_0$.

At the highest temperature considered, which was 684 K, the slopes of all three functions $\tilde{g}_0$, $\tilde{g}_1$, and $\tilde{g}_2$ on these log-log plots are very close to unity. This indicates that the regime has been reached where simple random-walk diffusion occurs. At lower temperatures, however, the slope is smaller, decreasing to a value close to 0.5 at most of the lower temperatures. This behavior is somewhat unexpected. While variation as $t$ is expected for free diffusion and variation as $t^{0.5}$ is predicted in the Rouse model [18], variation as intermediate powers of $t$ does not emerge from any simple theory.

*$T_g$ from the temperature dependence of mean squared displacement.* Figure 5 shows the mean squared displacements of Figs. 1 and 2 replotted as a function of temperature at different observation times for the three different cases, all of which show the same behavior. The characteristics of the mean squared displacements at low temperatures are distinctly different from those at high temperatures. The change in slope of the mean squared displacement as a function of temperature in all the three cases and for all of the four chosen observation times occurs around the same temperature. The mean squared displacement is proportional to T (which is expected for a harmonic oscillator) up to about 395 K, beyond which it increases far more rapidly with temperature. We then tentatively identify the glass transition temperature for our system to be $395 \pm 5$ K.
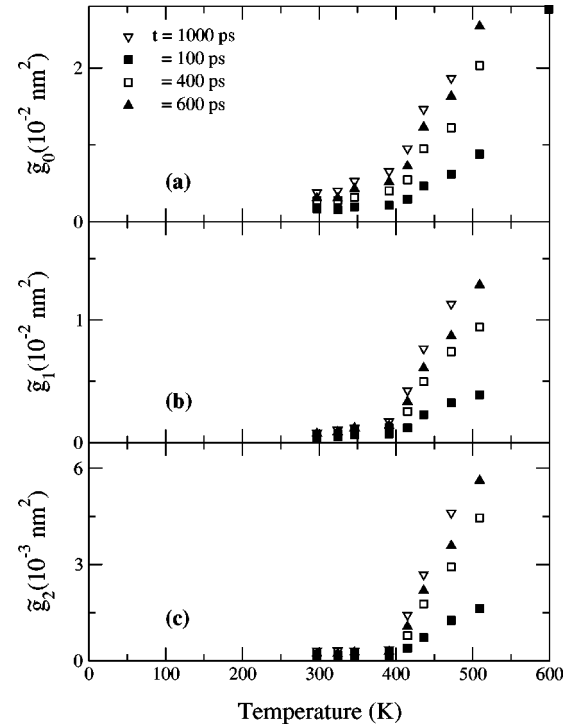
We can also make use of the reduced mean squared displacements, $\tilde{g}_0$, $\tilde{g}_1$, and $\tilde{g}_2$ to make a more refined determination of $T_g$. This time we plot in Fig. 6 values found at fixed times from Fig. 4 as functions of temperature. We now see a very clear transition that is common to the atomic, monomeric, and polymeric functions, but which is most precisely seen in the polymeric reduced mean squared displacement. The plots each consist of two linear regions that intersect at around $396 \pm 2$ K. We identify this temperature as $T_g$.

The fact that our numerical result for $T_g$ is in good agreement with the experimental value of about 397 K [19] must be taken as largely coincidental for two reasons. First: the force field used is not expected to be accurate to better than a few percent in an application like the present one, in which it is the differences in depth of adjacent potential wells that determine the diffusion rate. The second, and more important, reason is that the diffusion rate is expected to depend on the degree of polymerization, and our chains were comparatively short, consisting of only 15 monomer units. According to Fox and Flory [20], the value of $T_g$ should decrease linearly with inverse molecular weight. Ute *et al.* [19] suggest a value for the slope of this line of 9400 K on the basis of extrapolations of their calorimetric measurements. Applied to our system this would suggest a value for $T_g$ of about 340 K, making our result an overestimate of about 16%. It can be compared with some previous work by Soldera [4], who found $T_g$ for chains of 100 monomers to be 485 K, which is 25% larger than the experimental value of about 387 K. He attributed this high value of $T_g$ to the extremely rapid cooling rate used in the simulation, and also to his comparatively short simulation run of 110 ps. Soldera worked at constant
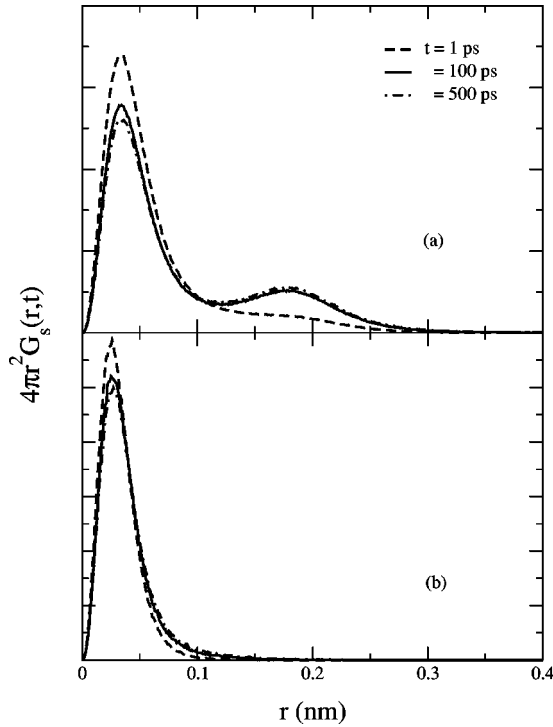
FIG. 7. The van Hove self-correlation function for T=297 K, the lowest temperature studied, shown for different values of the time $t$, for (a) hydrogen atoms only, and (b) monomeric center of mass.



FIG. 8. As in Fig 7, but for T=468 K, far above $T_g$.

pressure rather than constant volume, as his method was to find $T_g$ from the coefficient of the thermal expansion.

The significant aspect of the present paper is not the numerical value of $T_g$ predicted, as this is dependent on the type of force field used. The real strength of the technique used here lies in the unambiguous nature of the prediction obtained from the reduced mean squared displacement function $\tilde{g}(t)$. The subtraction of the harmonic component of the mean squared displacement prior to constructing the log-log plot as a function of time appears to be a powerful tool with which to extract new information.

*van Hove correlation function.* For temperatures below $T_g$, we note from Fig. 5 that the atomic mean squared displacement $g_0(t)$ increases much more rapidly with time than do either the monomeric or polymeric functions, $g_1(t)$ and $g_2(t)$. The small magnitude of the displacements suggests that some minor cooperative rearrangements of the constituent atoms within a monomer might be responsible. We, thus, require another tool with which to study this phenomenon.

Much useful information about the space and time dependence of atomic and monomeric motions can be found from the self-part of the van Hove space-time correlation function defined as

$$G_s(r,t) = \langle \delta(\mathbf{r} - \mathbf{r}_i(t) + \mathbf{r}_i(0)) \rangle, \quad (14)$$

where $\mathbf{r}_i(t)$ denotes the position of atom or molecule $i$ at time $t$ and $r = |\mathbf{r}|$. This gives us the probability density of finding an atom (monomer) at a distance $r$ at time $t$ if the atom (monomer) was observed at $r=0$ at time $t=0$.
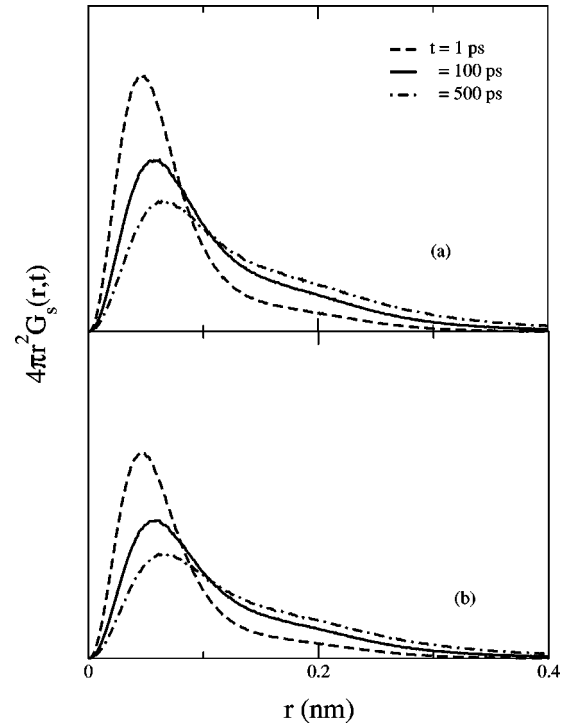
Figure 7 shows the values of $P(r,t) = 4\pi r^2 G_s(r,t)$ for (a) hydrogen atoms and (b) monomers at T=297 K, the lowest temperature studied. The van Hove function for the carbon atoms (not shown here) has the same single-peaked form as the monomer case and is not of interest for the present study. In both cases in Fig. 7, with increasing time the positions of the peaks do not shift, indicating that the diffusional motion is completely arrested at this temperature. For the case of the hydrogen atoms $P(r,t)$ consists of two well-defined peaks with time-independent positions.

The presence of a second peak in $P(r,t)$ is of particular significance, since it is usually cited as evidence of hopping processes. This has been confirmed for the case of soft-sphere binary liquids [21–25]. In polymeric liquids [26] the presence of hopping processes will modify the prediction of the simple mode-coupling theory in which these effects are neglected, and provides a possible mechanism for the blurring of the sharp glass transition predicted by the idealized mode-coupling theory [27,28]. The absence of a second peak has been taken as evidence that hopping process do not occur [8,28]. In our case, however, we interpret the second peak as resulting from the rotation of the $CH_3$ group, since it occurs at $r \approx 0.18$ nm, which is the distance between the H atoms in the $CH_3$ group. As expected, this feature is absent from the monomeric probability distribution. Bead-spring models of polymers will not show this distinction, which can only be seen from the atomistic van Hove correlation function.

Figure 8 shows the values of $P(r,t)$ at T=468 K, far above $T_g$. In this case the second peak for the hydrogen atoms has disappeared and the first peak for both cases is now moving towards large values of r as $t$ increases. At this temperature other additional degrees of freedom are present, and effects due to the rotation of the $CH_3$ group are no longer significant.

## VI. SUMMARY AND CONCLUSIONS

We have performed atomistic molecular dynamics simulation to examine the glass transition in syndiotactic PMMA. The model system consisted of 18 chains of PMMA, with degree of polymerization 15, with periodic boundary conditions applied. From the atomic trajectories that were obtained in the simulations, we calculated atomic, monomeric, and molecular mean squared displacements to characterize the dynamics of our polymer system at different length scales and in different time ranges.

A theoretical analysis indicated that it might be fruitful to subtract from the mean squared deviation the expected contribution from oscillatory motion. When this was done the remaining contribution, which is attributed to diffusive motion, showed a power-law behavior. The exponent for this power law was approximately 0.5 for $T < T_g$, and increased to unity at 684 K. A study of the self part of the van Hove correlation function for atomic motion indicated that rotation of methyl groups was a likely source of some of the low-temperature atomic motion.

Overall, our results indicate that molecular-dynamics simulations can provide useful information about the nature of the glass transition in polymers in computational runs of modest size. Use of an uncomplicated force field is helpful in reaching the diffusive regime with modest computational resources. Subtraction of the oscillatory contribution to the motion is a useful tool with which to reveal the time variation of diffusive displacements.

### ACKNOWLEDGMENTS

[1] R.O. Ebewele, *Polymer Science and Technology* (CRC Press, New York, 2000).

[2] C. Bennemann, W. Paul, K. Binder, and B. Dunweg, Phys. Rev. E **57**, 843 (1998).

[3] C.A. Angell, Science **267**, 1924 (1995).

[4] A. Soldera, Macromol. Symp. **133**, 21 (1998).

[5] J. Han, R.H. Gee, and R.H. Boyd, Macromolecules **27**, 7781 (1994).

[6] C.F. Fan, T. Cagin, W. Shi, and K.A. Smith, Macromol. Theory Simul. **6**, 83 (1997).

[7] M.D. Ediger, C.A. Angel, and S.R. Nagel, J. Phys. Chem. **100**, 13200 (1996).

[8] R.-J. Roe, J. Chem. Phys. **100**, 1610 (1994).

[9] J. Norberg and L. Nilsson, Proc. Natl. Acad. Sci. U.S.A. **93**, 10 173 (1996).

[10] A. Abragam, in *Low-Temperature Physics*, edited by C. Dewitt, B. Dreyfus, and P. G. de Gennes (Gordon and Breach, New York, 1962), p. 491.

[11] S.L. Mayo, B.D. Olafson, and W.A. Goddard III, J. Phys. Chem. **94**, 8897 (1990).

[12] D. Rigby, H. Sun, and B.E. Eichinger, Polym. Int. **44**, 311 (1997).

[13] M. Tsige, M.P. Mahajan, C. Rosenblatt, and P.L. Taylor, Phys. Rev. E **60**, 638 (1999).

[14] T.P. Doerr and P.L. Taylor, Int. J. Mod. Phys. C **10**, 415 (1999).

[15] T.P. Doerr and P.L. Taylor, Mol. Cryst. Liq. Cryst. Sci. Technol., Sect. A **330**, 491 (1999).

[16] CERIUS² Simulation Tools User's Reference (Molecular Simulations Inc., Cambridge, 1994).

[17] W. Paul, K. Binder, D.W. Heermann, and K. Kremer, J. Chem. Phys. **95**, 7726 (1991).

[18] P.E. Rouse, J. Chem. Phys. **21**, 127 (1953).

[19] K. Ute, N. Miyatake, and K. Hatada, Polymer **36**, 1415 (1995).

[20] T.G. Fox and P.J. Flory, J. Appl. Phys. **21**, 581 (1950).

[21] B. Bernu, J.-P. Hansen, Y. Hiwatari, and G. Pastore, Phys. Rev. A **36**, 4891 (1987).

[22] H. Miyagawa, Y. Hiwatari, B. Bernu, and J.-P. Hansen, J. Chem. Phys. **88**, 3879 (1988).

[23] J.-N. Roux, J.-L. Barrat, and J.-P. Hansen, J. Phys.: Condens. Matter **1**, 7171 (1989).

[24] J.L.- Barrat, J.-N. Roux, and J.-P. Hansen, Chem. Phys. **149**, 197 (1990).

[25] J.L.- Barrat and J.-N. Roux, J. Non-Cryst. Solids **131-133**, 255 (1991).

[26] J.-L. Barrat and M.L. Klein, Annu. Rev. Phys. Chem. **42**, 23 (1991).

[27] W. Kob and H.C. Andersen, Phys. Rev. E **47**, 3281 (1993).

[28] W. Kob and H.C. Andersen, Phys. Rev. E **51**, 4626 (1995).